Self-assembled monolayers of benzylmercaptan and *para*-cyanobenzylmercaptan on gold: surface infrared spectroscopic characterization†

K. Rajalingam,[a] L. Hallmann,[a] T. Strunskus,[bc] A. Bashir,[c] C. Wöll*[c] and F. Tuczek*[a]

Received 10th November 2009, Accepted 8th February 2010
First published as an Advance Article on the web 5th March 2010
DOI: 10.1039/b923628g

Self-assembled monolayers (SAMs) on gold substrates were prepared from benzylmercaptan (BM) and *para*-cyanobenzylmercaptan (pCBM), and the resulting surfaces were investigated using conventional infrared reflection-absorption spectroscopy (IRRAS) as well as polarization modulation infrared reflection-absorption spectroscopy (PM-IRRAS). IRRAS data are analyzed by comparison with transmission IR spectra and theoretical (DFT) simulations. The spectroscopic results indicate the presence of well-ordered monolayers of BM and pCBM with an orientation perpendicular to the surface. IRRAS and PM-IRRAS data are compared to each other and the respective merits of both methods are discussed.

Introduction

The vibrational spectroscopic characterization of molecules adsorbed on surface has gained considerable interest in the recent years.[1] A well-established technique in this regard is infrared reflection-absorption spectroscopy (IRRAS) which allows obtaining high-quality infrared spectra of monolayers of organic molecules deposited on metal surfaces. A characteristic feature of this method is the surface selection rule, which states that only the vibrations with a component of the transition dipole moment aligned perpendicular to the surface plane can interact with the incident light and contribute to the infrared spectrum.[2–5] This way, IRRAS also provides information about the orientation of the surface adsorbed molecules. The inherent surface selection rule as well as the sensitivity renders this method particularly suitable for the structural and spectroscopic characterization of self-assembled monolayers (SAMs) which have important applications in molecular electronics and catalysis.[6–10]

With respect to the latter subject, transition-metal containing SAMs are particularly useful.[11–14] These systems can be assembled on metal surfaces in two ways. The first method involves the direct attachment of transition-metal complexes with suitable ligands, for example, thiol terminated ligands on gold surfaces.[15,16] The second method employs the reaction of transition-metal containing precursors with suitably pre-functionalized surfaces.[17–20] For the latter approach, bifunctional linkers such as *para*-cyanobenzylmercaptan (pCBM) are required. In this molecule, the thiol group binds to the gold surface whereas the nitrile group can coordinate to a transition-metal complex. Importantly, the lateral spacing between adjacent nitrile groups can be varied by diluting pCBM with unsubstituted benzylmercaptan (BM), thus generating SAMs with a defined density of nitrile groups protruding from a flat surface. By this method, the steric demand of different transition-metal complexes can also be accounted for. The attachment of metal complexes can then be conveniently monitored by determining the C–N stretching frequency by IRRAS. Moreover, the cyano terminated molecules are excellent Raman reporters. Employing these properties, the role of pCBM-functionalized nanoparticles, *e.g.*, in cell studies has been demonstrated earlier.[21] The molecular structures of BM and pCBM as well as models of BM-, pCBM- and mixed BM/pCBM-SAMs are shown in Fig. 1 and 2.

Recently we have investigated the formation of self-assembled monolayers of BM and pCBM on Au(111) surfaces

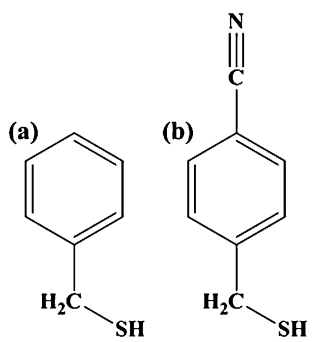

Fig. 1 Molecular structures of (a) BM and (b) pCBM.

[a] *Institut für Anorganische Chemie, Christian-Albrechts Universität Kiel, Max-Eyth-Straße 2, 24098 Kiel, Germany*
[b] *Lehrstuhl für Materialverbünde, Technische Fakultät der Christian-Albrechts-Universität zu Kiel, Kaiserstraße 2, 24143 Kiel, Germany*
[c] *Institut für Funktionelle Grenzflächen, Forschungszentrum Karlsruhe, 76021 Karlsruhe, Germany*

† Electronic supplementary information (ESI) available: Carbon–hydrogen stretching frequency region of bulk IR and Raman of BM liquid and calculated IR and Raman of BM (Fig. S1); carbon–hydrogen stretching frequency region of bulk IR and Raman of pCBM and calculated IR and Raman of pCBM (Fig. S2); negative absorption bands in the region from 2400 to 2000 cm^{-1} (Fig. S3). See DOI: 10.1039/b923628g

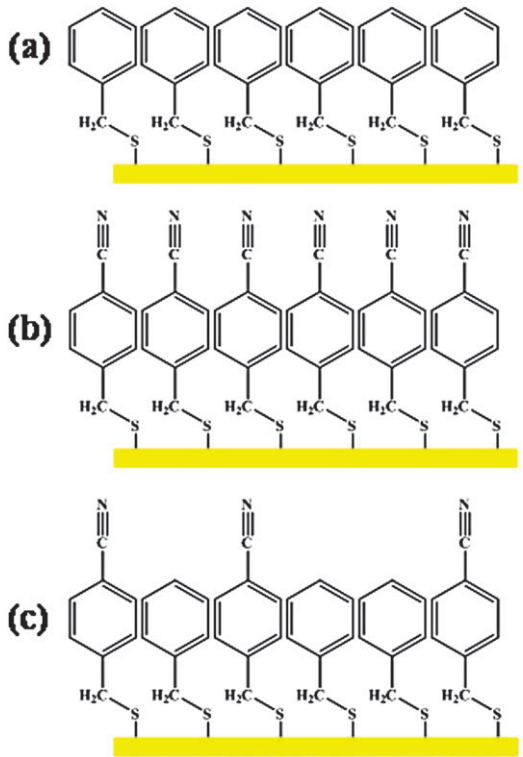

Fig. 2 Models of the structures of (a) BM-SAM, (b) pCBM-SAM and (c) the mixed SAM of BM and pCBM adsorbed on gold.

with a combination of X-ray photoelectron spectroscopy (XPS), near-edge X-ray absorption fine structure (NEXAFS) and scanning tunneling microscopy (STM).[22] Thereby it was found that BM as well as pCBM form well-ordered monolayers with the molecules oriented almost perpendicular to the surface. Specifically, BM forms a $(\sqrt{3} \times \sqrt{3})$ R30^0 structure whereas pCBM forms a slightly different c(7 × 7) hexagonal structure. It was also established that BM and pCBM form mixed monolayers with no phase separation.

Herein we present infrared spectroscopic investigations on these systems using IRRAS and PM-IRRAS. These techniques provide information that is complementary to STM, XPS and NEXAFS. In particular, they also allow determining the orientation of the BM and pCBM molecules with respect to the surface normal, which in our previous study has mainly been inferred from NEXAFS. To this end, IRRAS and PM-IRRAS data of BM and pCBM have been recorded. While the spectra resulting from both techniques should in principle be identical, data evaluation differs for both techniques, leading to slightly different results in practice. For IRRAS measurements a clean and suitable background sample is necessary whereas in the PM-IRRAS technique there is no need for a reference sample. Though the IRRAS instrument is continuously purged with nitrogen gas, absorptions from the surrounding atmosphere are also detected. On the other hand, PM-IRRAS serves as a suitable method to eliminate bands from atmospheric absorptions. The only disadvantage of PM-IRRAS is that the data are more difficult to interpret because of the complex baseline correction. The methodological goal of this paper is to compare the IRRAS and PM-IRRAS data with each other on two well-defined systems in order to obtain an impression of the reliability of the information obtained with either technique. The experimental spectra are also compared with theoretical simulations obtained from DFT-based vibrational frequencies and intensities. The implications of the results with respect to the vibrational characterization of SAMs are discussed.

Experimental

Chemicals

Benzylmercaptan (BM) was obtained from Fluka and was used as received. *para*-Cyanobenzylmercaptan (pCBM) was synthesized using a procedure as described in ref. 23. Ethanol (Roth; analytical grade, 99.8%) was used as received.

Synthesis of *para*-cyanobenzylmercaptan (pCBM)

pCBM was prepared using *para*-cyanobenzylbromide and thiourea.[23] *para*-Cyanobenzylbromide (9.8 g, 0.05 mole) and thiourea (3.8 g, 0.05 mole) were dissolved in 40 ml of ethanol and the solution was heated to about 100 °C under reflux for 1 h. The excess of solvent was removed by pumping and the residual creamy white thiuronium salt was washed with ethyl acetate. The dried solid substance was dissolved in distilled water. Prior to use, distilled water was degassed using argon. To the solution 10% sodium hydroxide solution was slowly added with rapid stirring at room temperature. The sodium salt of *para*-cyanobenzylmercaptan was obtained as a white precipitate. Then, concentrated hydrochloric acid was added with rapid stirring. By means of solvent extraction with ether, the final compound was separated and dried over anhydrous sodium sulfate. The procedure is shown in Fig. 3. The purity of the compound was checked by NMR.

Monolayer preparation

Self-assembled monolayers (SAMs) of BM and pCBM were prepared by immersing the Au(111) substrates into a 1 mM ethanolic solution of the respective thiol at room temperature. After 24 h of immersion, the sample was removed from the solution, thoroughly rinsed with copious amounts of the solvent (ethanol) and finally dried in a stream of nitrogen gas.[22] For comparison, the SAM samples were also additionally rinsed with tetrahydrofuran (THF).

Gold substrates

The polycrystalline gold substrates were prepared by physical vapor deposition of 5 nm of titanium (99.8%, Chempur) and subsequently 100 nm of gold (99.995%, Chempur) onto polished (100) oriented silicon wafers (Wacker) in an evaporation chamber operated at a base pressure of 10^{-7} mbar.[20]

Bulk IR

IR of pCBM dispersed in KBr was recorded on Bruker VERTEX 70 FT-IR spectrometer in transmission mode using a DTGS detector. IR of BM (liquid) was recorded with a sample cell with calcium fluoride windows.

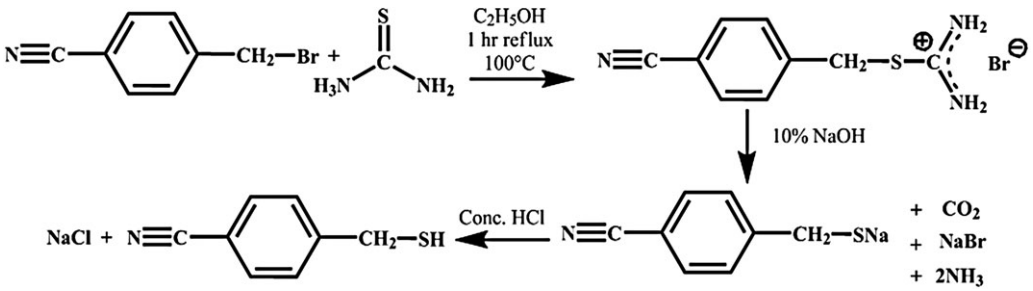

Fig. 3 Synthesis of *para*-cyanobenzylmercaptan.

IRRAS and PM-IRRAS

Surface-vibrational data were recorded with a Bruker VERTEX 70 FT-IR spectrometer equipped with a Polarization Modulation Accessory (PMA) 50 unit (Bruker Optik GmbH, Ettlingen, Germany) which allows recording both IRRAS and PM-IRRAS data. With this setup IRRA and PM-IRRA spectra can be recorded from 4000 down to 750 cm^{-1}. IRRAS data were collected with a liquid nitrogen cooled MCT detector and a horizontal reflection unit for grazing incidence (Bruker A518). A p-polarized beam at an incident angle of 80° to the surface normal was used for measurements. All spectra were recorded with 4 cm^{-1} resolution. The sample chamber was purged with dry nitrogen gas before and during measurements. SAMs of perdeuterated hexadecanethiol ($C_{16}D_{33}SH$) on gold were used as background samples in these experiments.

PM-IRRAS data were collected with the PMA 50 accessory using a liquid nitrogen-cooled MCT detector. Spectra were measured with a resolution of 4 cm^{-1} and the angle of incidence was 82°. Each spectrum contains 2048 averaged spectra. The PEM maximum efficiency was set for the half-wave retardation at 2900 cm^{-1} for analysis of the CH stretching bands, at 1100 cm^{-1} for analysis of the CN stretching mode and at 1500 cm^{-1} for analysis of the bands in the region below 1800 cm^{-1}.

IR data processing

The bulk IR of BM and pCBM were used without any baseline correction. The processing of IRRAS and PM-IRRAS data was carried out using the OPUS software Version 6.5 (Bruker, Germany). The baseline correction of the resulting IRRAS data was done by the rubber band method in an interactive mode. PM-IRRAS data have been processed by the implicit removal of the Bessel function by manual baseline correction.

Calculation details

The vibrational frequencies of pCBM and BM were calculated using a commercial program package, Gaussian 03.[24,25] DFT calculations were performed using the B3LYP (Becke-3-Parameter-Lee–Yang–Parr) functional together with a 6-31++G(d,p) basis set.[26,27] After geometry optimizations, theoretical frequencies were calculated. No negative frequencies were encountered. In the case of pCBM, the theoretical frequencies were scaled by a factor of 0.9678, which was obtained by normalizing the theoretical value to the experimental value for the ring modes (experimental 1606 cm^{-1}, theoretical 1659 cm^{-1}). The frequencies of BM were scaled by a factor of 0.9677. This normalization factor was obtained by comparing the theoretical and experimental value for the ring modes [experimental value/theoretical value = 1601 cm^{-1}/1654 cm^{-1} = 0.9677]. The vibrational modes were assigned by means of visual examination using the GaussView program.

Results and analysis

SAM of BM and pCBM

The BM and pCBM SAMs were prepared according to the procedures described above and subsequently investigated with IRRAS and PM-IRRAS. For both compounds, DFT calculations were performed. Furthermore, bulk KBr-pellet IR data of BM and pCBM were recorded in order to aid the assignment of the vibrational bands.

IRRAS of BM SAM

Fig. 4 shows the high frequency regions of the IR spectra recorded for the benzylmercaptan (BM) SAM and a KBr pellet prepared from pure BM along with the theoretical spectrum obtained from a DFT calculation. In Fig. 5, the corresponding mid- to low energy parts of the vibrational spectra are presented. Spectral assignments of all bands are based on a comparison between experimental (IRRAS/bulk) and theoretical data and are collected in Table 1.

C–H stretching region. The bulk spectrum of BM exhibits intense bands at 3084, 3062 and 3027 cm^{-1} denoted 2, 3 and 4

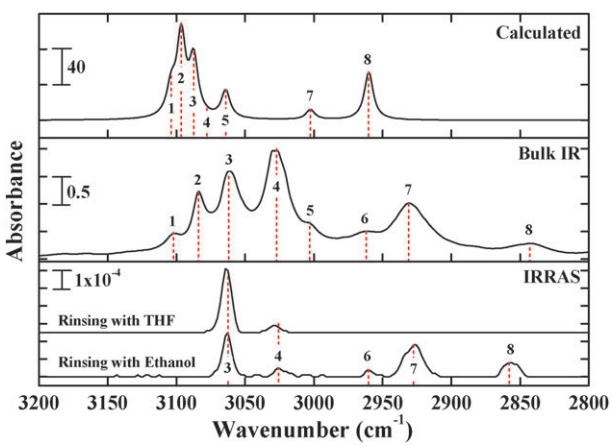

Fig. 4 High-frequency regions of infrared spectroscopic data of BM SAM, bulk BM in KBr and the calculated IR spectrum of BM.

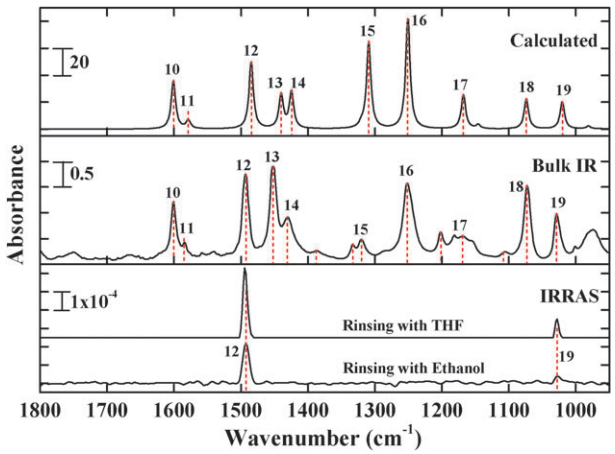

Fig. 5 Mid- to low-frequency regions of infrared spectroscopic data of BM SAM, bulk BM in KBr and the calculated IR spectrum of BM.

in Fig. 4. In the Wilson notation, these vibrations are assigned to ν_{20b}, ν_2 and ν_{20a}, respectively.[28] Calculated frequencies for ν_{20b}, ν_2 and ν_{20a} are 3097, 3087 and 3078 cm^{-1}. The bulk IR spectrum in addition exhibits vibrations at 3102 and 3003 cm^{-1} (denoted as 1 and 5, respectively) which are also assigned to aromatic C–H stretches (calculated frequencies: 3104 and 3064 cm^{-1}, respectively). In the IRRAS data, two C–H stretching vibrations of the aromatic ring in the BM molecule are observed at 3062 and 3026 cm^{-1} (Fig. 4). The presence of only two bands in the SAM IRRAS is a consequence of the IRRAS surface selection rule; *i.e.*, IR bands with transition dipole moment (TDM) oriented parallel to a metal surface are absent, bands with TDMs neither parallel nor perpendicular to the surface stay visible but are attenuated in intensity and bands with TDMs that are exactly perpendicular to the surface are most intense. For most of the vibrations of BM, the orientation of the TDM with respect to the surface plane is neither exactly parallel nor exactly perpendicular (marked with / in Table 1).

The aromatic stretches can be distinguished from the aliphatic CH_2 stretching bands with the aid of calculated data. In the IRRA spectrum of the sample prepared conventionally, *i.e.* by rinsing with ethanol, the CH_2 stretches appear at 2927 and 2858 cm^{-1}. In the bulk spectrum, they are found at 2931 and 2843 cm^{-1}. These bands are assigned to the antisymmetric and symmetric C–H vibration, respectively. In addition to these two peaks, the IRRA spectrum exhibits another peak at 2960 cm^{-1}. This peak is also observed in the bulk spectrum at around 2962 cm^{-1}. The assignment of this band is not obvious. A comparison of the bulk infrared data with the bulk Raman data reveals more information. For benzylmercaptan, five CH aromatic ring stretches and two CH_2 stretches are theoretically predicted. The experimental data clearly indicate that, in addition to these vibrations, the bulk liquid exhibits bands at 2960 cm^{-1} (more intense in IR) and 2980 cm^{-1} (more intense in the Raman; data provided in the ESI).† The peak at around 2960 cm^{-1} has been attributed to a combination of vibrations in the lower frequency region.[29]

Remarkably, the two CH_2 stretches and the 2960 cm^{-1} peak are absent in IRRAS of the BM SAM after thorough rinsing with tetrahydrofuran (THF). The corresponding spectra are included in Fig. 4 and 5. In the high frequency region there are now only the two bands present that derive from the aromatic stretches of BM. This finding appears to indicate that the bands below 3000 cm^{-1} (*i.e.*, the aliphatic stretches) derive from some impurity adsorbed on the SAM surface. On the other hand, literature IRRAS data on SAMS of 4-picolylmercaptan also show the presence of C–H vibrations

Table 1 Infrared vibrational band assignments for benzylmercaptan. The vibrational frequencies (wavenumbers, cm^{-1}) obtained from the KBr pellet, calculated, IRRAS and PMIRRAS are given in the first four columns. In the fifth column, the orientation of the transition dipole moment (TDM) is given with respect to the surface plane (perpendicular: ⊥, parallel: ∥ and neither totally parallel nor totally perpendicular: /). The assignment of the bands has been made in the seventh column. Wilson notation is given in brackets

Peak number	Bulk	Calculated	IRRAS	PM-IRRAS	TDM	Assignment
1	3102	3104	—	—	/	(CH_{ring}) stretching
2	3084	3097	—	—	/	(CH_{ring}) stretching (ν_{20b})
3	3062	3087	3062	3063	/	(CH_{ring}) stretching (ν_2)
4	3027	3078	3026	—	/	(CH_{ring}) stretching (ν_{20a})
5	3003	3064	—	—	/	(CH_{ring}) stretching
6	2962	—	2960	—	—	Combination modes
7	2931	3002	2927	2928	/	(CH_2) asymmetric stretching
8	2843	2960	2858	2858	/	(CH_2) symmetric stretching
9	2565	2598	—	—	⊥	(SH) stretching
10	1601	1601	—	—	⊥	(CC_{ring}) stretching; (CH_{ring}) deformation (ν_{8a})
11	1585	1579	—	—	/	(CC_{ring}) stretching; (CH_{ring}) deformation (ν_{8b})
12	1493	1484	1493	1495	⊥	(CC_{ring}) & (CH_{ring}) deformation (ν_{19a})
13	1452	1440	—	—	∥	(CH_2) & (CH_{ring}) bending (ν_{19b})
14	1431	1424	—	—	/	(CH_2) & (CH_{ring}) bending
15	1320	1309	—	—	/	(CC_{ring}) deformation; (CH_2) wagging
16	1252	1251	—	—	/	(CH_{ring}) deformation; (CH_2) wagging
17	1169	1168	—	—	/	(CH_{ring}) deformation; (CH_2) wagging
18	1073	1074	—	—	∥	(CC_{ring}) bending; (CH_2) & (SH) wagging
19	1029	1020	1028	1028	⊥	(CC_{ring}) bending (ν_{18a})
20	976	982	—	—	/	(CC_{ring}) deformation
21	908	908	—	—	∥	(CC_{ring}) bending; (CH_2) twisting
22	758	786	—	—	/	(CH_2) & (SH) wagging; (CC_{ring}) deformation
23	698	711	—	—	∥	(CC_{ring}) & (CH_{ring}) bending; (CH_2) twisting
24	679	667	—	—	∥	(CC_{ring}) & (CH_{ring}) bending; (CH_2) twisting

of the methylene group.[30] For this reason and in view of the fact that the CH_2 vibrations are also found for pCBM (see below) the IRRAS data for the SAMs of BM prepared by both methods (rinsing with ethanol and rinsing with THF) are shown.

C–C stretching region. In the bulk spectrum, the BM molecule exhibits six C–C stretching bands. The first one is found at 1601 cm^{-1} and a second about 15 cm^{-1} lower in frequency. According to Wilson notation, they are assigned as ν_{8a} and ν_{8b}.[31] Two other C–C stretching modes are observed at 1493 and 1452 cm^{-1}, labelled as ν_{19a} and ν_{19b}. The fifth and sixth modes are observed at 1320 and 1252 cm^{-1}. The C–C ring bending mode can be found at 1029 cm^{-1}. Calculated and observed frequencies are again collected in Table 1. The IRRAS data of the BM SAM, in contrast, only reveal the presence of one intense peak at 1493 cm^{-1} and another peak at 1028 cm^{-1} with much lower intensity (Fig. 5, ''rinsing with ethanol''). The presence of only two peaks and the changes in relative intensity when compared to the bulk spectrum can be explained by the surface selection rule (*vide supra*). The intense peak at 1493 cm^{-1} is assigned to the C–C and C–H ring deformation and the peak at 1028 cm^{-1} is assigned to the C–C ring bending. In both cases, the TDM is oriented perpendicular to the gold surface and parallel to the molecular axis of the benzene ring (Fig. 6). After rinsing with THF, the two peaks at 1493 and 1028 cm^{-1} both appear with somewhat higher intensity, suggesting that the quality of the SAM is improved by this procedure (see above).

S–H stretching frequency. The SH stretching frequency of the thiol dispersed in KBr is observed at 2565 cm^{-1}. The SH vibrational band observed at 2565 cm^{-1} in the bulk is absent in the IR spectra recorded for the BM SAM (Fig. 7). This indicates that the BM thiol adsorbs on gold as thiolate.

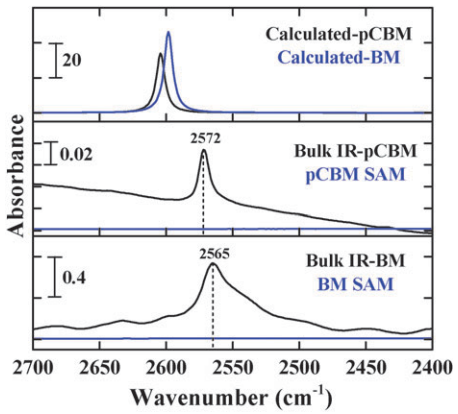

Fig. 7 SH stretching regions of infrared spectroscopic data of pCBM and BM (calculated, bulk and SAM IRRAS).

Apart from the peaks in the positive direction, few absorption bands in the negative direction are observed in the region from 2400 to 2000 cm^{-1} (data supplied as ESI).† The band at around 2360 cm^{-1} corresponds to the asymmetric stretching vibration of CO_2 in the sample compartment of the IR spectrometer. Other negative bands are due to the perdeuterated hexadecanethiol ($C_{16}D_{33}SH$) reference SAM. The CD_2 symmetric and asymmetric stretching vibrations are observed at 2075 and 2193 cm^{-1}, respectively. The CD_3 symmetric and asymmetric stretching vibrations are observed at 2089 and 2222 cm^{-1}, respectively.

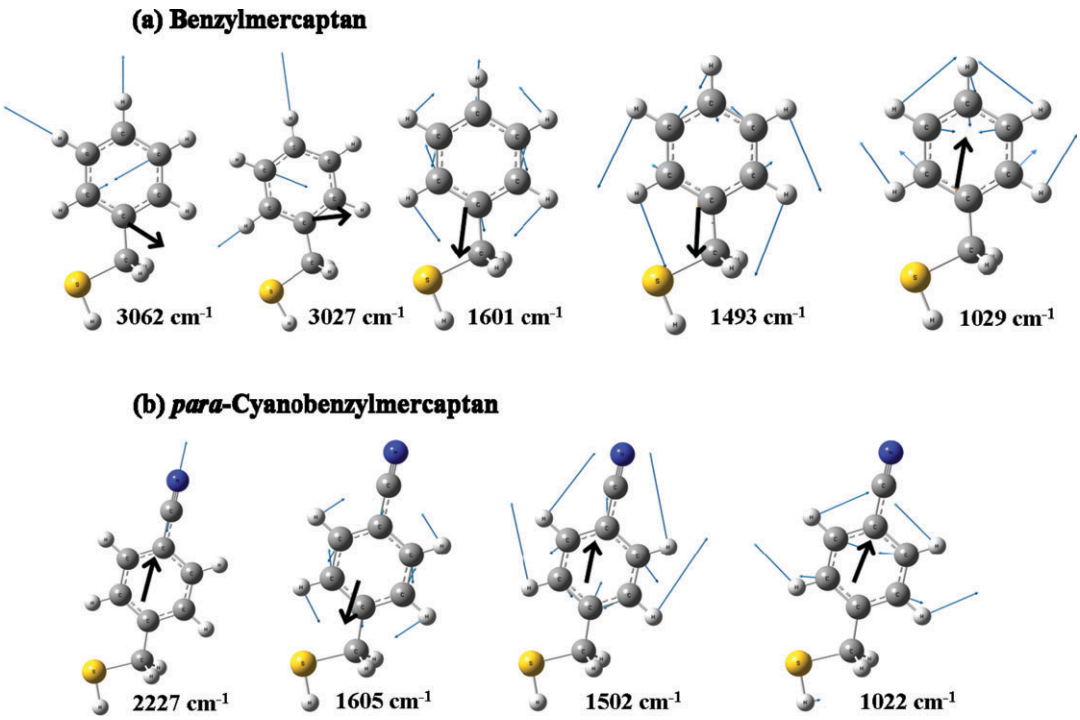

Fig. 6 Orientation of the dipole derivative unit vector for (a) benzylmercaptan and (b) *para*-cyanobenzylmercaptan deduced using GaussView software. The thin arrows represent the displacement vectors and bold arrows show the dipole derivative unit vector.

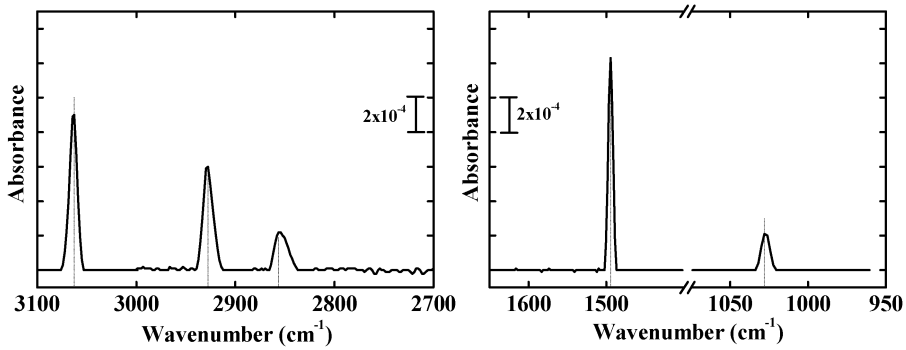

Fig. 8 PM-IRRAS data of BM SAM.

PM-IRRAS of BM SAM. The PM-IRRAS spectra of BM in the high- and mid- to low frequency regions are displayed in Fig. 8. In the C–H stretching region, the PM-IRRAS spectrum is quite similar to its "normal" IRRAS counterpart in Fig. 4. Distortions from Gaussian band shapes in the PM-IRRAS spectra are due to the background subtraction procedure. In the lower frequency region, the PM-IRRAS spectrum exhibits the 1028 cm^{-1} band with a higher intensity than the IRRAS spectrum of the sample obtained by rinsing with ethanol.

IRRAS of pCBM SAM

The high frequency regions of the IR spectra recorded for a *para*-cyanobenzylmercaptan (pCBM) SAM and a KBr pellet prepared from pure pCBM are shown along with the spectrum obtained from a DFT calculation in Fig. 9. In Fig. 10, the corresponding mid- to low energy parts of the vibrational spectra of pCBM are presented. The peak positions and assignments of all bands are collected in Table 2.

C–H stretching region. Most conspicuously, the intensity of the aromatic C–H stretches of pCBM (peaks 1–4) is dramatically decreased in the bulk-IR with respect to BM while the intensity of the aliphatic C–H stretches is about the same as for BM (Fig. 9, middle). This is also reflected in the IRRA spectra of pCBM which do not show any aromatic C–H

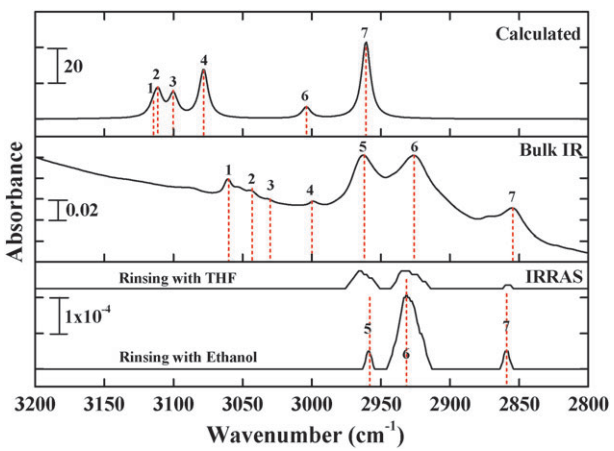

Fig. 9 High-frequency regions of infrared spectroscopic data of pCBM SAM, bulk pCBM in KBr and the calculated IR spectrum of pCBM.

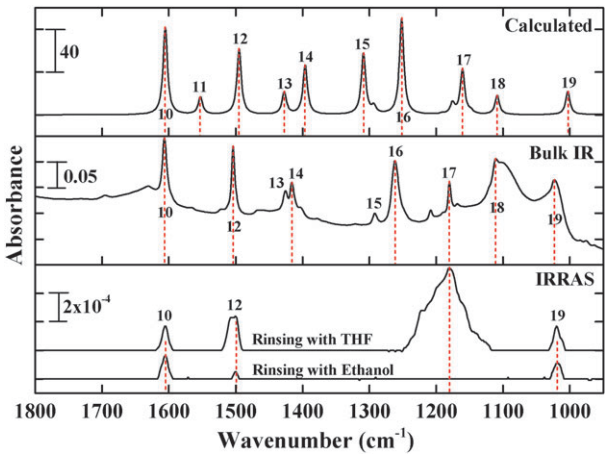

Fig. 10 Mid- to low-frequency regions of infrared spectroscopic data of pCBM SAM, bulk pCBM in KBr and the calculated IR spectrum of pCBM.

stretches, in contrast to the BM SAM. In particular, the intense 3062 cm^{-1} band observed in the case of BM is not observed for pCBM. Introduction of the cyano group in the *para* position thus appears to have "quenched" the C–H stretching vibrations of the benzene ring. The calculations qualitatively predict a decrease in relative intensity of the aromatic stretches, but not as extreme as observed.

In the aliphatic C–H stretching region, both the bulk-IR and the IRRA spectrum of the pCBM SAM prepared conventionally (*i.e.*, by rinsing with ethanol) exhibit three bands (5,6 and 7). Again, theory predicts the presence of only two bands in this region, suggesting that one of the observed bands is a combination mode (*vide supra*). By comparison with vibrational data from BM, we conclude that the bands at 2931 and 2859 cm^{-1} are the antisymmetric and symmetric C–H stretching vibrations, respectively, whereas the 2958 cm^{-1} band is a combination mode. A look at the experimental bulk-IR and -Raman spectrum of pCBM, however, reveals that the situation is even more complicated: in a region where only two bands are predicted, comparison of the IR and Raman spectra indicates the presence of up to seven distinct bands (data provided in the ESI).† The detailed assignments of these bands are not clear; in analogy to the case of BM we conclude that five of these features must be overtones and/or combination bands.

Table 2 Infrared vibrational band assignments for *para*-cyanobenzylmercaptan

Peak number	Bulk	Calculated	IRRAS	PM-IRRAS	TDM	Assignment
1	3060	3115	—	—	/	(CH_{ring}) stretching (ν_2)
2	3043	3111	—	—	/	(CH_{ring}) stretching
3	3031	3100	—	—	/	(CH_{ring}) stretching (ν_{20a})
4	3000	3078	—	—	/	(CH_{ring}) stretching
5	2963	—	2958	2956	—	Combination modes
6	2926	3004	2931	2929	/	(CH_2) asymmetric stretching
7	2856	2961	2859	2858	/	(CH_2) symmetric stretching
8	2572	2604	—	—	⊥	(SH) stretching
9	2227	2259	2234	2231	⊥	(CN) stretching
10	1606	1606	1605	1605	⊥	(CC_{ring}) stretching; (CH_{ring}) deformation (ν_{8a})
11	—	1553	—	—	/	(CC_{ring}) stretching; (CH_{ring}) deformation (ν_{8b})
12	1504	1495	1501	1502	⊥	(CC_{ring}) & (CH_{ring}) deformation (ν_{19a})
13	1426	1427	—	—	/	(CH_2) bending
14	1417	1396	—	—	∥	(CC_{ring}) & (CH_{ring}) deformation
15	1290	1308	—	—	/	(CC_{ring}) deformation; (CH_2) wagging
16	1261	1251	—	—	/	(CH_2) & (SH) wagging
17	1179	1160	—	—	/	(CC_{ring}) deformation; (CH_2) wagging
18	1110	1109	—	—	/	(CC_{ring}) bending
19	1022	1003	1020	1020	⊥	(CH_{ring}) deformation (ν_{18a})
20	849	911	—	—	/	(SH) wagging
21	826	888	—	—	∥	(CC_{ring}) bending; (CH_2) twisting
22	803	790	—	—	∥	(CC_{ring}) bending; (CH_2) twisting
23	734	742	—	—	/	(CH_2) & (SH) wagging; (CC_{ring}) deformation
24	661	685	—	—	∥	(CC_{ring}) & (CH_{ring}) bending; (CH_2) twisting

After thorough rinsing of the pCBM SAM with tetrahydrofuran (THF), the two CH_2 stretches and the 2958 cm^{-1} peak are both broadened and reduced in intensity (*cf.* Fig. 9). This again might indicate that the bands below 3000 cm^{-1} (*i.e.*, the aliphatic stretches) derive from some impurity adsorbed on the SAM surface. In contrast to the BM SAM, however, the peaks do not disappear completely upon rinsing with THF. This could mean that there is some intrinsic intensity of these vibrations in the pCBM SAM which is, however, weak. This would be in agreement with the TDM of these vibrations being slightly tilted out of the surface plane. On the other hand, rinsing with THF in the case of the pCBM SAM also introduces a broad and intense peak in the mid-IR region (see below) which corresponds to an impurity. It is well-known that THF intercalates into SAMs on gold,[32,33] and for these reasons rinsing with THF appears to deteriorate the quality of the pCBM SAM, in contrast to the case of BM. The influence of ethanol and THF on the quality of SAMs is under constant debate in the literature.[34,35]

S–H stretching frequency. The SH stretching for the bulk pCBM is observed at 2572 cm^{-1}. The absence of the SH stretching band in the SAM spectra shows that the pCBM is bound to the gold surface through the sulfur atom (Fig. 7).

CN stretching frequency. The CN group is linear and in plane with the benzene ring. The CN stretching mode is polarized perpendicular to the surface and can be easily identified by a strong, sharp band at 2227 cm^{-1}. The nitrile vibrational band is observed at 2234 cm^{-1} in the IRRAS of the pCBM SAM (Fig. 11). Only a small shift is observed when compared to the bulk. This indicates that the cyano group is free on top of the SAM surface. Infrared spectroscopic evidence thus reveals that the cyano group is not involved in surface bonding.

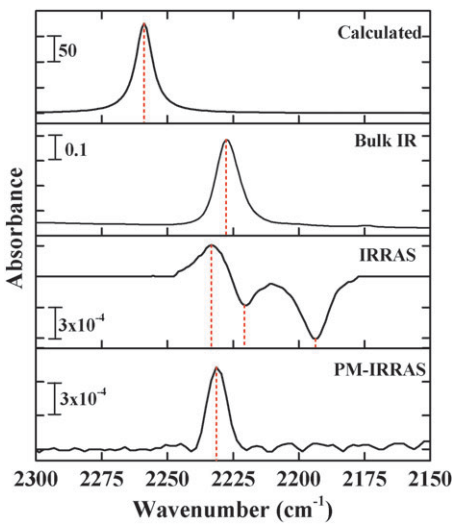

Fig. 11 Cyano stretching regions of infrared spectroscopic data of pCBM SAM (IRRAS and PM-IRRAS), bulk pCBM in KBr and the calculated IR spectrum of pCBM.

C–C stretching region. There are two C–C ring stretching/C–H ring deformation bands in the bulk-IR spectrum which are located at 1606 and 1504 cm^{-1} (Fig. 10); another C–H ring bending mode can be found at 1022 cm^{-1}. In the pCBM SAM, the C–C/C–H ring deformation and C–H ring bending vibrations are observed at 1605, 1501 and 1020 cm^{-1}, respectively (peaks 10, 12 and 19 in Fig. 10). Fig. 6 shows that the TDMs of these vibrations are oriented perpendicular to the gold surface. In the SAM obtained by rinsing with THF, peak 12 is broadened and, in addition, a broad and intense feature appears at 1180 cm^{-1} which derives from an impurity. We therefore anticipate that the quality of the corresponding SAM is lower than of that obtained by rinsing with ethanol.

Interestingly, the IRRAS spectrum of pCBM exhibits an intense peak at 1605 cm^{-1} whereas this peak is absent in the IRRAS spectrum of BM (it is, however, present in the bulk-IR spectrum of BM). The 1600 cm^{-1} band (ν_{8a}) corresponds to a symmetric combination of C–H bends with respect to a mirror plane perpendicular to the *z*-axis of BM (the *z*-axis being defined as the vector between the benzyl group at C_1 and C_4). Although the transition dipole moment of this particular normal mode is perpendicular to the surface (thus rendering this vibration IRRAS-active), its absolute value may become zero due to an accidental cancellation of C–H bending motions at C_2 and C_6 on the one hand and C_3 and C_5 on the other. This we observe in case of BM. For pCBM the situation is different in that nonvanishing, effective transition dipole moment results, and in this case the vibration is observed at 1605 cm^{-1}. The situation is different for the 1500 cm^{-1} mode (ν_{19a}) which represents an antisymmetric combination of C–H bending motions with respect to a mirror plane perpendicular to *z*. In this case the C–H bending vibrations of C_2 and C_6 on the one hand and C_3 and C_5 on the other add up, and the resulting transition-dipole moment is only weakly dependent upon a substitution at the C_4 position. Thus the vibration is IRRAS-active for both BM and pCBM, in agreement with the observation. Examples for the observation of such phenomena in bulk IR spectroscopy can be found in the literature.[36–38]

PM-IRRAS of pCBM

The PM-IRRAS spectra of pCBM in the high- and mid- to low frequency regions are displayed in Fig. 12. Apart from slight differences in relative intensities and band shapes, these spectra are quite similar to their IRRAS counterparts in Fig. 9 and 10. The negative bands in the IRRAS data are due to the deuterated background. PM-IRRAS employs the effect that on metal surfaces, at high angles of incidence only p-polarized radiation was absorbed and nearly no absorbances are observed with s-polarized light. This change in absorbance intensities offers the possibility to measure the difference between spectra collected with incident s- and p-polarized infrared radiation. Thus, PM-IRRAS offers the possibility to remove interferences from the gas phase absorptions as well as avoids the need of a clean background. With respect to the C–N stretch which falls into the region of C–D vibrations and is thus difficult to record, PM-IRRAS clearly shows the advantage of not relying on a background spectrum (Fig. 12).

Discussion and conclusions

In the present study, self-assembled monolayers (SAMs) of benzylmercaptan (BM) and *para*-cyanobenzylmercaptan (pCBM) were investigated with IRRAS and PM-IRRAS. A comparison of the band positions for the SH vibrations between bulk samples in KBr and the SAMs showed that the mercaptans are adsorbed on the Au(111) surface through the sulfur along with loss of mercaptan hydrogen as no SH bands are observed in the SAM spectra. Of particular interest in the lower frequency region are the peak positions for the ring stretching modes which can be compared to the KBr spectra of the respective mercaptan.

Several groups have investigated benzyl mercaptan SAM on gold.[39–45] BM has been employed to study the rates of electron transport in a metal-SAM-metal junction[46] and also in molecular electronics.[47] Earlier studies from our group clearly showed the formation of well-ordered, upright oriented BM SAM on Au(111).[22] This is supported by the present IRRAS investigations. In agreement with the result of Tao *et al.*,[48] a ring-stretching vibration is found at 1493 cm^{-1} for BM. For pCBM this peak is shifted to 1501 cm^{-1}; in addition a second intense peak appears at 1605 cm^{-1}. The nitrile CN stretch of pCBM is observed at 2234 cm^{-1}. Both mercaptans exhibit a peak at $\sim$1020 cm^{-1} in the IRRAS spectra which is assigned to a C–C ring bending vibration, in accordance with the previous studies.[44] Based on the surface selection rule of IRRAS, the intensity of out-of-plane ring modes for an orientation of the ring of BM and pCBM perpendicular to the surface vanishes because the transition dipole moment of these modes is oriented parallel to the surface. As we cannot see any peak belonging to such modes we conclude that these mercaptans are oriented perpendicular to the surface or with a small tilt angle to the surface normal, in agreement with the results from our NEXAFS study.[22]

In order to obtain further information on the presence of aliphatic C–H stretches in the IRRA spectra of BM and pCBM, the influence of the SAM preparation on the observed spectra has been investigated. In principle, the transition-dipole moments of the symmetric and antisymmetric stretches of the CH_2 group are only slightly tilted with respect to the surface, and the intensities of the corresponding bands in IRRAS should therefore be weak. For BM, a complete suppression of these bands has in fact been achieved by rinsing the SAMs with THF, in agreement with Tao *et al.*[48] For

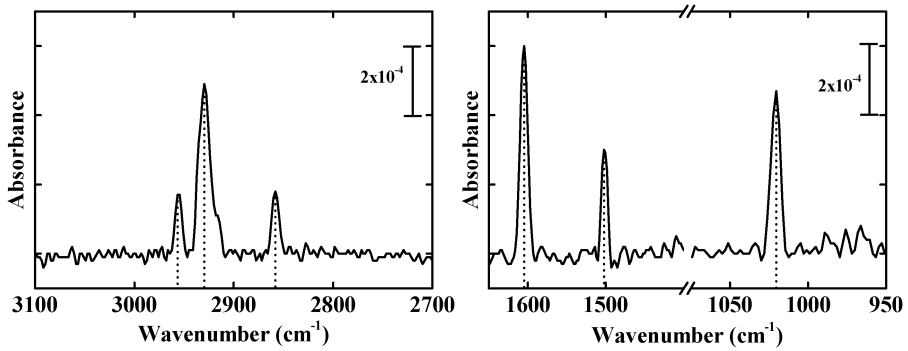

Fig. 12 PM-IRRAS data of pCBM SAM.

pCBM, the same procedure leads to a significant intensity decrease of these bands; on the other hand, a broad and intense peak emerged which derives from an impurity (maybe intercalated THF). For the sake of completeness and because CH_2 vibrations are observed in IRRA spectra of related systems in the literature,[30] we decided to present the spectra of both samples obtained by rinsing with ethanol and by rinsing with THF.

The comparison of IRRAS and PM-IRRAS spectra in the present study indicates that both methods give very similar spectra. In particular, good agreement with respect to band positions is observed whereas relative intensities and bandwidths slightly vary. The latter finding is due to the background subtraction procedure in PM-IRRAS, which renders this method less straightforward to apply than "normal" IRRAS. On the other hand, PM-IRRAS is particularly useful when the reference spectrum exhibits bands in spectral regions where interesting vibrational features of the sample are located (*e.g.*, the CN-stretch in pCBM) or when application of a reference spectrum is not possible. In a forthcoming study we will apply the methodology outlined in this paper to investigate the attachment of metal complexes to SAMs of BM and pCBM.

Acknowledgements

F.T. and K.R. thank Prof. Dr A. Terfort, Goethe-Universität Frankfurt, for providing the perdeuterated hexadecanethiol. Special thanks are due to Prof. G. Wittstock and Dr I. Zawisza from University of Oldenburg for preliminary measurements and fruitful discussions. Bruker Optik GmbH, Ettlingen, Germany is gratefully acknowledged for technical support. Financial support from SFB 677 is gratefully acknowledged.

References

1 F. Hoffmann, Infrared reflection-absorption spectroscopy of adsorbed molecules, *Surf. Sci. Rep.*, 1983, **3**, 107–192.
2 R. G. Greenler, Infrared study of adsorbed molecules on metal surfaces by reflection techniques, *J. Chem. Phys.*, 1966, **44**, 310–315.
3 R. Arnold, A. Terfort and C. Wöll, Determination of Molecular Orientation in Self-Assembled Monolayers Using IR Absorption Intensities: The Importance of Grinding Effects, *Langmuir*, 2001, **17**, 4980–4989.
4 V. G. Gregoriou and S. E. Rodman, Vibrational Spectroscopy of Thin Organic Films, in *Handbook of Vibrational Spectroscopy*, ed. P. R. Griffiths and J. Chalmers, John Wiley & Sons Ltd, 2002, ch. 4, pp. 2670–2693.
5 P. Hollins, Surface infrared spectroscopy, *Vacuum*, 1994, **45**, 705–714.
6 C. A. Mirkin and M. A. Ratner, Molecular electronics, *Annu. Rev. Phys. Chem.*, 1992, **43**, 719–754.
7 J. M. Tour, Molecular Electronics. Synthesis and Testing of Components, *Acc. Chem. Res.*, 2000, **33**, 791–804.
8 J. C. Love, L. A. Estroff, J. K. Kriebel, R. G. Nuzzo and G. M. Whitesides, Self-Assembled Monolayers of Thiolates on Metals as a Form of Nanotechnology, *Chem. Rev.*, 2005, **105**, 1103–1169.
9 X. M. Li, J. Huskens and D. N. Reinhoudt, Reactive self-assembled monolayers on flat and nanoparticle surfaces, and their application in soft and scanning probe lithographic nanofabrication technologies, *J. Mater. Chem.*, 2004, **14**, 2954–2971.
10 M. C. Daniel and D. Astruc, Gold Nanoparticles: Assembly Supramolecular Chemistry, Quantum-Size-Related Properties, and Applications toward Biology, Catalysis, and Nanotechnology, *Chem. Rev.*, 2004, **104**, 293–346.
11 V. Huc, Transition metal catalysts for molecular motors: towards molecular lithography, *J. Phys.: Condens. Matter*, 2006, **18**, S1909–S1926.
12 K. Hara, R. Akiyama, S. Takakusagi, K. Uosaki, T. Yoshino, H. Kagi and M. Sawamura, Self-Assembled Monolayers of Compact Phosphanes with Alkanethiolate Pendant Groups: Remarkable Reusability and Substrate Selectivity in Rh Catalysis, *Angew. Chem.*, 2008, **120**, 5709–5712.
13 S. Berner, S. Biela, G. Ledung, A. Gogoll, J. Bäckvall, C. Puglia and S. Oscarsson, Activity boost of a biomimetic oxidation catalyst by immobilization onto a gold surface, *J. Catal.*, 2006, **244**, 86–91.
14 T. Belser, M. Stöhr and A. Pfaltz, Immobilization of Rhodium Complexes at Thiolate Monolayers on Gold Surfaces: Catalytic and Structural Studies, *J. Am. Chem. Soc.*, 2005, **127**, 8720–8731.
15 K. Hara, K. Iwahashi, S. Takakusagi, K. Uosaki and M. Sawamura, Construction of self-assembled monolayer terminated with N-heterocyclic carbene–rhodium(I) complex moiety, *Surf. Sci.*, 2007, **601**, 5127–5132.
16 J. R. deSousa, I. C. N. Diogenes, M. L. A. Temperini, F. A. M. Sales, S. O. Pinheiro, R. N. C. Filho, J. S. d. Junior and I. S. Moreira, Synthesis, characterization, and SAMs electroactivity of ruthenium complexes with sulfur containing ligands, *J. Organomet. Chem.*, 2007, **692**, 3691–3699.
17 K. D. Dronavajjala, R. Rajagopalan, S. Uppili, A. Sen, D. L. Allara and H. C. Foley, A Simple Technique To Grow Polymer Brushes Using *in situ* Surface Ligation of an Organometallic Initiator, *J. Am. Chem. Soc.*, 2006, **128**, 13040–13041.
18 T. Vallant, W. Simanko, H. Brunner, U. Mayer, H. Hoffmann, R. Schmid, K. Kirchner, R. Svagera, G. Schügerl and M. Ebel, Comparing Reactivities of Metal Complexes in Solution and on Surfaces by IR Spectroscopy and Time-Resolved *in situ* Ellipsometry, *Organometallics*, 1999, **18**, 3744–3749.
19 J. Luo and S. S. Isied, Ruthenium Tetraammine Chemistry of Self-Assembled Monolayers on Gold Surfaces: Substitutionand Reactivity at the Monolayer Interface, *Langmuir*, 1998, **14**, 3602–3606.
20 K. Rajalingam, T. Strunskus, A. Terfort, R. A. Fischer and C. Wöll, Metallization of a Thiol-Terminated Organic Surface Using Chemical Vapor Deposition, *Langmuir*, 2008, **24**, 7986–7994.
21 D. C. Kennedy, L. Tay, R. K. Lyn, Y. Rouleau, J. Hulse and J. P. Pezacki, Nanoscale Aggregation of Cellular β_2—Adrenergic Receptors Measured by Plasmonic Interactions of Functionalized Nanoparticles, *ACS Nano*, 2009, **3**, 2329–2339.
22 L. Hallmann, A. Bashir, T. Strunskus, R. Adelung, V. Staemmler, C. Wöll and F. Tuczek, Self-Assembled Monolayers of Benzylmercaptan and p-Cyanobenzylmercaptan on Au(111) Surfaces: Structural and Spectroscopic Characterization, *Langmuir*, 2008, **24**, 5726–5733.
23 M. Bellas, D. L. Tuleen and L. Field, Organic disulfides and related substances. XXII. Substituted benzyl 2-(N-decylamino) ethyl disulfide hydrochlorides. A possible neighboring-group effect involving sulfur, *J. Org. Chem.*, 1967, **32**, 2591–2595.
24 M. J. Frisch, G. W. Trucks, H. B. Schlegel, G. E. Scuseria, M. A. Robb, J. R. Cheeseman, J. A. Montgomery, T. Vreven, K. N. Kudin, J. C. Burant, J. M. Millam, S. S. Iyengar, J. Tomasi, V. Barone, B. Mennucci, M. Cossi, G. Scalmani, N. Rega, G. A. Petersson, H. Nakatsuji, M. Hada, M. Ehara, K. Toyota, R. Fukuda, J. Hasegawa, M. Ishida, T. Nakajima, Y. Honda, O. Kitao, H. Nakai, M. Klene, X. Li, J. E. Knox, H. P. Hratchian, J. B. Cross, C. Adamo, J. Jaramillo, R. Gomperts, R. E. Stratmann, O. Yazyev, A. J. Austin, R. Cammi, C. Pomelli, J. W. Ochterski, P. Y. Ayala, K. Morokuma, G. A. Voth, P. Salvador, J. J. Dannenberg, V. G. Zakrzewski, S. Dapprich, A. D. Daniels, M. C. Strain, O. Farkas, D. K. Malick, A. D. Rabuck, K. Raghavachari, J. B. Foresman, J. V. Ortiz, Q. Cui, A. G. Baboul, S. Clifford, J. Cioslowski, B. B. Stefanov, G. Liu, A. Liashenko, P. Piskorz, I. Komaromi, R. L. Martin, D. J. Fox, T. Keith, M. A. Al-Laham, C. Y. Peng, A. Nanayakkara, M. Challacombe, P. M. W. Gill, B. Johnson, W. Chen, M. W. Wong, C. Gonzalez and J. A. Pople, *GAUSSIAN 03*, Gaussian Inc., Pittsburgh PA, 2003.
25 A. Frisch, A. B. Nielsen and A. J. Holder, *Gaussview Users Manual*, Gaussian Inc., 2000.

26 C. Lee, W. Yang and R. G. Parr, Development of the Colle-Salvetti correlation-energy formula into a functional of the electron density, *Phys. Rev. B: Condens. Matter*, 1988, **37**, 785–789.
27 A. D. Becke, Density-functional thermochemistry. III. The role of exact exchange, *J. Chem. Phys.*, 1993, **98**, 5648–5652.
28 E. B. Wilson, A Partial Interpretation of the Raman and Infrared Spectra of Benzene, *Phys. Rev.*, 1934, **46**, 146–147.
29 S. E. Wiberley, S. C. Bunce and W. H. Bauer, Carbon–Hydrogen stretching frequencies, *Anal. Chem.*, 1960, **32**, 217–221.
30 J. Liu, L. Stratmann, S. Krakert, M. Kind, F. Olbrich, A. Terfort and C. Wöll, IR spectroscopic characterization of SAMs made from a homologous series of pyridine disulfides, *J. Electron Spectrosc. Relat. Phenom.*, 2009, **172**, 120–127.
31 D. A. Zimmerman, J. L. Koenig and H. Ishida, Infrared spectroscopic analysis of poly(*p*-phenylene sulfide), *Spectrochim. Acta, Part A*, 1995, **51**, 2397–2409.
32 W. R. T. Barden, S. Singh and P. e. Kruse, Roughening of Gold Atomic Steps Induced by Interaction with Tetrahydrofuran, *Langmuir*, 2008, **24**, 2452–2458.
33 B. Berron and G. K. Jennings, Loosely Packed Hydroxyl-Terminated SAMs on Gold, *Langmuir*, 2006, **22**, 7235–7240.
34 D. A. Krapchetov, H. Ma, A. K. Y. Jen, D. A. Fischer and Y. L. Loo, Solvent-Dependent Assembly of Terphenyl- and Quaterphenyldithiol on Gold and Gallium Arsenide, *Langmuir*, 2005, **21**, 5887–5893.
35 Y. Tai, A. Shaporenko, H. T. Rong, M. Buck, W. Eck, M. Grunze and M. Zharnikov, Fabrication of Thiol-Terminated Surfaces Using Aromatic Self-Assembled Monolayers, *J. Phys. Chem. B*, 2004, **108**, 16806–16810.
36 E. D. Schmid and R. D. Topsom, Raman Intensity and Conjugation, 5. A Quantitative Relationship between Raman Intensity and the Length of Conjugation and an Analysis of the Raman Intensities of Some Substituted Benzenes and Biphenyls, *J. Am. Chem. Soc.*, 1981, **103**, 1628–1632.
37 I. K. Korobeinicheva, O. M. Fugaeva and G. G. Furin, Influence of fluorine atoms on intensity of aromatic ring vibrations in raman spectra of fluorobenzenes and pentafluoro-substituted derivatives of benzene, *Bull. Acad. Sci. USSR, Div. Chem. Sci. (Engl. Transl.)*, 1987, **36**, 1634–1637.
38 G. Z. Mamatov and M. R. Yagudaev, Integral intensities of the infrared bands due to the stretching vibrations of the aromatic ring in the 1620–1480 cm^{-1} range, *Zhurnal Prikladnoi Spektroskopii*, 1968, **8**, 825–829.
39 T. Baunach and D. M. Kolb, The electrochemical characterisation of benzyl mercaptan-modified Au(111): Structure and copper deposition, *Anal. Bioanal. Chem.*, 2002, **373**, 743–748.
40 F. Wrochem, F. Scholz, A. Yasuda and J. M. Wessels, Probing Structure and Molecular Conductance in Highly Ordered Benzyl Mercaptan Monolayers, *J. Phys. Chem. C*, 2009, **113**, 12395–12401.
41 H. H. Jung, Y. D. Won, S. Shin and K. Kim, Molecular Dynamics Simulation of Benzenethiolate and Benzyl Mercaptide on Au(111), *Langmuir*, 1999, **15**, 1147–1154.
42 J. Y. Gui, D. A. Stern, D. G. Frank, F. Lu, D. C. Zapien and A. T. Hubbard, Adsorption and Surface Structural Chemistry of Thiophenol, Benzyl Mercaptan, and Alkyl Mercaptans. Comparative Studies at Ag(111) and Pt(111) Electrodes by Means of Auger Spectroscopy, Electron Energy Loss Spectroscopy, Low-Energy Electron Diffraction, and Electrochemistry, *Langmuir*, 1991, **7**, 955–963.
43 S. Joo and Y. Kim, Surface-enhanced Raman scattering study of benzyl mercaptide and benzyl isocyanide on gold and silver nanocolloid surfaces, *Colloids Surf., A*, 2004, **234**, 117–122.
44 E. J. Sturrock, Q. Chen, P. H. Borchardt and N. V. Richardson, Coverage dependent change in orientation for the adsorption of benzyl mercaptan on Au(111), *J. Electron Spectrosc. Relat. Phenom.*, 2004, **135**, 127–134.
45 N. Nishi, D. Hobara, M. Yamamoto and T. Kakiuchi, Orientation of o-, m-, and p-Methylbenzylmercaptans Adsorbed on Au(111) Probed by Broad-Bandwidth Sum Frequency Generation Spectroscopy, *Langmuir*, 2003, **19**, 6187–6192.
46 R. E. Holmlin, R. Haag, M. L. Chabinyc, R. F. Ismagilov, A. E. Cohen, A. Terfort, M. A. Rampi and G. M. Whitesides, Electron Transport through Thin Organic Films in Metal-Insulator-Metal Junctions Based on Self-Assembled Monolayers, *J. Am. Chem. Soc.*, 2001, **123**, 5075–5085.
47 R. Liu, S. H. Ke, H. U. Baranger and W. Yang, Intermolecular effect in molecular electronics, *J. Chem. Phys.*, 2005, **122**, 44703.
48 Y. T. Tao, C. C. Wu, J. Y. Eu, W. L. Lin, K. C. Wu and C. H. Chen, Structure Evolution of Aromatic-Derivatized Thiol Monolayers on Evaporated Gold, *Langmuir*, 1997, **13**, 4018–4023.